Flow Over an Airfoil with Jets

Yuriy A. Krassin*
Moscow, USSR

The flow over an airfoil with jets is considered in two cases: where the Bernoulli constants of the jets and freestream are equal, and where they are different. The first case concerns entering jets and the second escaping jets. Complex variables are used. In the first case, the flow is represented by a source-vortex singularity at the airfoil. In the second, vortex sheets on the jet boundaries are added to the previous system. Vortex strengths are defined by the vertical jet momentum and source strengths by the horizontal jet momentum. Simple equations are obtained for the jet lift augmentation, which depends on the total heads of the jet and the freestream, the initial jet angle, jet momentum flux, and jet flow rate. These parameters can be chosen to be optimum for minimal takeoff and landing distances.

Nomenclature

A = aspect ratio
B = Bernoulli constant of freestream
b_ℓ^* = Bernoulli constant of jet number ℓ
C_L = lift coefficient
C_{L0} = lift coefficient without jet influence
c = airfoil chord
c_D, c_{D0} = total and profile drag coefficients
c_J = jet thrust coefficient
$c_{J\ell}$ = jet thrust coefficient number ℓ
f = wheel rolling friction coefficient
h_∞ = thickness of jet at downstream infinity
$\mathbf{J}$ = jet momentum flux vector
J = absolute value of jet momentum flux
J_ℓ = jet momentum flux at the exit or entrance number ℓ
K = efficiency factor
k = source-vortex distance parameter
L = lift
M = resultant moment
N = takeoff horsepower
P = resultant force
P_x, P_y = projection of P on X and Y axis, respectively
Q_j = volume flow rate of jet number j
q_ℓ = source number ℓ
R = radial coordinate
r = radius of the circle G in the ζ plane
s = wing span
T = thrust or drag, projection of the resultant force on X axis (Fig. 2)
U_∞ = absolute value of stream velocity at infinity
V = fluid velocity vector
V_n = fluid velocity component normal to arc length mn
V_∞ = fluid velocity of the jet at infinity
w = complex potential
x, y = components of complex variable z
z = complex variable
α = angle of attack
Γ = circulation of velocity vector on path surrounding airfoil
γ_ℓ = vortex component of singularity ℓ
ζ = complex variable
η = angle of a jet
η_j = angle of jet j at entrance or exit
θ = angular coordinate of point in complex plane
ξ = component of the complex variable
ρ = fluid density
ψ = component of the complex variable

Superscripts

$\bar{(\ )}$ = conjugated complex value
$(\ )^*$ = sign of jet Bernoulli constant

Subscripts

j,k,ℓ = numbers of a jet or singularity
L = lift
$L0$ = lift without supercirculation
n = necessary value
∞ = at infinity
$+\infty$ = at downstream infinity
$-\infty$ = at upstream infinity

Introduction

THE first theoretical work dealing with the airfoil lift increment generated by jets entering into and escaping from an airfoil was published in the late 1930's.[1] In this work, the problem of the lift of a cylinder with one source and one sink located on its contour was resolved. The basic work in this field was published by Spence.[2] In this publication, the lift increment generated by the vertical component of a jet momentum flux at the jet exit from an airfoil was obtained. Spence also obtained simple formulas for the lift increment calculations.[3] Since the mid-1950's many experimental and theoretical works considering this matter have been published, one of the latest being Ref. 4. A very interesting monograph published by Soviet scientist Shurigin[5] resolved some problems concerning jets of finite thickness using Riemann surfaces. In the present article, simple formulas, convenient for STOL aircraft characteristics calculations, are obtained.

Absence of Discontinuity in Velocity at Boundaries

Assume an ideal, incompressible, weightless fluid and consider a two-dimensional problem of steady flow over an airfoil S. The latter has m entering and $n-m$ escaping jets and is located in an infinite flow. The fluid of the stream and of the jets have the same density. The stream has velocity $U_\infty e^{i\alpha}$ at infinity. The positive measure of the angle α is counterclockwise. Figure 1 shows this kind of flow over an airfoil S with $m=1$ and $n-m=1$. The plane of the drawing is identified as

Received Feb. 27, 1988; revision received Aug. 1, 1988.

*Independent Researcher.

one of the complex variable $z = x + iy$. The channel shown in Fig. 1 as a dotted line, which connects the entering and escaping jets in real structures such as a jet engine, is replaced by a partition. In cavities fde and klg, the singularities, namely source vorticies, are located at points A_k and A_j. A negative source component is used for the entering jet and positive one for the escaping jet. The angle of the jet is considered equal to the angle of its momentum flux J,

$$J = \int_{mn} VV_n \, ds \tag{1}$$

where the arc length mn in most cases is part of the equipotential line crossing the jet.

The positive measure of the jet angle η is clockwise and $0 \leq |\eta| \leq \pi$. The jet direction entering or leaving the airfoil is considered to coincide with the jet momentum flux at the nozzle or with the nozzle direction. The volume flow rates of the entering and escaping jets are constant, as

$$Q_j = V_{+\infty j} h_{+\infty j} \qquad j = m+1 \quad m+2,...n \tag{2}$$

$$Q_k = -V_{-\infty k} h_{-\infty k} \qquad k = 1,2,3...m \tag{3}$$

and those of the entering jets are negative by definition. Taking as a base the geometric similarity between the jet escaping from the nozzle and the jet generated by the singularity, namely a source vortex, assign, for any entering or escaping jet, a source vortex located at a point A_ℓ. These singularities have a source component in a form

$$q_\ell = J_\ell \cos(\eta_\ell + \alpha) \frac{\operatorname{sgn} Q_\ell}{\rho U_\infty} \qquad \ell = 1,2,3,...m,m+1,...n \tag{4}$$

and a vortex component

$$\gamma_\ell = -J_\ell \sin(\eta_\ell + \alpha) \frac{\operatorname{sgn} Q_\ell}{\rho U_\infty} \qquad \ell = 1,2,3,...m,m+1,...n \tag{5}$$

where $\operatorname{sgn} Q_\ell = +1$ if $Q_\ell \geq 0$ and $\operatorname{sgn} Q_\ell = -1$ if $Q_\ell < 0$. This replacement of a real jet by a jet from a source vortex leads to the absence of the tangent discontinuity of the velocity at the boundaries between the jet and the stream. The discontinuity would occur if the Bernoulli constants of the jets and of the stream were unequal. The airfoil S may now be considered an infinite plate $-\frac{1}{2} \leq z \leq +\frac{1}{2}$, $z = x_1 + iy_1$ (Fig. 2).

Now map the plate exterior to the exterior of circle G with radius r in the plane ζ, $\zeta = \xi + i\psi$ by means of the analytical function $z = \zeta + (r^2/\zeta)$ so that point $z = \frac{1}{2}$ maps into the point $\zeta = r$ and a point z at infinity into point ζ at infinity. Since $[dz/d\zeta]_{\zeta \to \infty} = 1$ and $dw/d\zeta = U_\infty e^{-i\alpha}$, where w is the complex potential, it follows that $r = \frac{1}{4}$ and sources and vortices at the points A_ℓ of the plane z will become sources and vortices of the same strength which are now located at points a_ℓ of the plane ζ. Here $a_\ell = R_\ell e^{i\theta_\ell}$. The complex velocity of the flow in the plane ζ is

$$\frac{dw}{d\zeta} = U_\infty e^{-i\alpha}\left(1 - \frac{r^2 e^{2i\alpha}}{\zeta^2}\right) + \frac{1}{2i\pi}\Gamma\frac{1}{\zeta} + \frac{1}{2\pi}\sum_{\ell=1}^{m+n}\frac{q_\ell}{\zeta - a_\ell} + \frac{1}{2\pi}\sum_{\ell=1}^{m+n}\frac{q_\ell}{\zeta - b_\ell} - \frac{1}{2\pi}\sum_{\ell=1}^{m+n}\frac{q_\ell}{\zeta} + \frac{1}{2i\pi}\sum_{\ell=1}^{m+n}\frac{\gamma_\ell}{\zeta - a_\ell} - \frac{1}{2i\pi}\sum_{\ell=1}^{m+n}\frac{\gamma_\ell}{\zeta - b_\ell} \tag{6}$$

where $b_\ell = r^2/\bar{a}_\ell$ and $\bar{a}_\ell = a_{\ell x} - ia_{\ell y}$ if $a_\ell = a_{\ell x} + a_{\ell y}$. The condition of finite velocity at point $z = \frac{1}{2}$ of the plate $-\frac{1}{2} \leq z \leq +\frac{1}{2}$ gives $[dw/d\zeta]_{\zeta = r} = 0$. Under this condition,

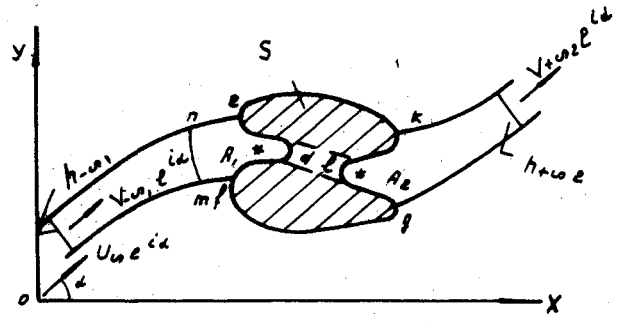

Fig. 1 Flow over an airfoil with jets.

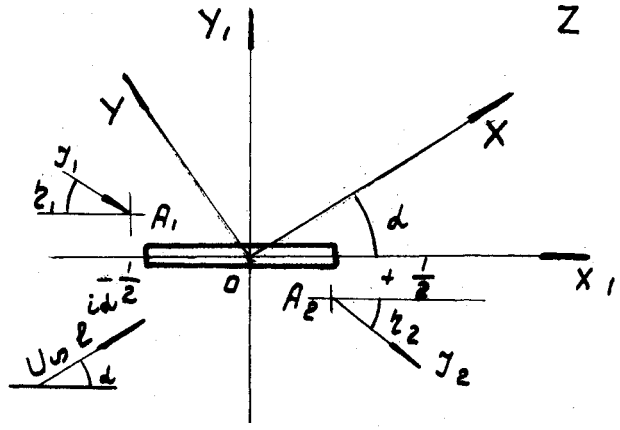

Fig. 2 Flow over the plate with jets.

taking account that

$$\frac{1}{r - a_\ell} + \frac{1}{r - b_\ell} = \frac{1}{r}\left(1 + i\frac{2rR_\ell \sin\theta_\ell}{r^2 - 2rR_\ell \cos\theta_\ell + R_\ell^2}\right) \tag{7}$$

$$\frac{1}{r - a_\ell} - \frac{1}{r - b_\ell} = \frac{r^2 - R_\ell^2}{r(r^2 - 2rR_\ell \cos\theta_\ell + R_\ell^2)} \tag{8}$$

Eq. (6) gives

$$\Gamma = -4\pi r U_\infty \sin\alpha + \sum_{\ell=1}^{m+n} q_\ell \frac{2rR_\ell \sin\theta_\ell}{r^2 - 2rR_\ell \cos\theta_\ell + R_\ell^2} + \sum_{\ell=1}^{m+n}\gamma_\ell \frac{R_\ell^2 - r^2}{r^2 - 2rR_\ell \cos\theta_\ell + R_\ell^2} \tag{9}$$

To calculate the resultant force P on the plate $-\frac{1}{2} \leq z \leq +\frac{1}{2}$ or on G, consider that the source vortices located at the points A_ℓ (or a_ℓ) are added to the plate (or to G) and apply the formula of Chapligin-Blasius. In that case,

$$\bar{P} = P_x - iP_y = \frac{i\rho}{2}\oint_{K_1}\left(\frac{dw}{dz}\right)^2 dz = \frac{i\rho}{2}\oint_K \left(\frac{dw}{d\zeta}\right)^2 \frac{d\zeta}{dz}\, d\zeta \tag{10}$$

where K_1 is a closed curve that surrounds the place and all the points A_ℓ, $\ell = 1,2,...m,...n$ and K a curve that surrounds G and all the points a_ℓ.

The resultant moment is

$$M = Re\left[-\frac{\rho}{2}\oint_{K_1}\left(\frac{dw}{dz}\right)^2 z\, dz\right] = Re\left[-\frac{\rho}{2}\oint_K \left(\frac{dw}{d\zeta}\right)^2 z(\zeta)\frac{d\zeta}{dz}\, d\zeta\right] \tag{11}$$

Calculating

$$\left(\frac{dw}{d\zeta}\right)^2 \frac{d\zeta}{dz} = \left(\frac{dw}{d\zeta}\right)^2\left[1 + \frac{r}{2}\left(\frac{1}{\zeta - r} - \frac{1}{\zeta + r}\right)\right]$$

where $dw/d\zeta$ is in accordance with Eq. (6), observe that every expression of types

$$\frac{q_k q_j}{(\zeta - a_k)(\zeta - a_j)}, \quad \frac{q_k \gamma_j}{(\zeta - a_k)(\zeta - b_j)}$$

$$\frac{q_k}{\zeta^2(\zeta - a_k)}, \quad \frac{q_k}{(\zeta - a_k)(\zeta - r)}$$

gives a pair of simpler fractions $1/(\zeta - a_k)$ and $-1/(\zeta - a_j)$ of different sign. Thus, the sum of their residues over the closed curve K or K_1 is zero.

Omitting the intermediate tedious derivations, the result is

$$T = -\rho U_\infty \sum_{\ell=1}^{m+n} q_\ell \tag{12}$$

$$L = -\rho U_\infty \Gamma \tag{13}$$

Equation (12) may be obtained also from application of the linear momentum theorem to the control volume contained between cross sections far in front of and behind the airfoil, under the condition that the initial jet momentum flux in the cavities (fde and clg of Fig. 1) is zero. (The jet momentum flux of the nozzle is not an initial one. See also Ref. 6.) Taking into account the same considerations as in the resultant force calculation, the resultant moment becomes

$$M = -Re\left\{\zeta\pi_i\left[2U_\infty^2 r^2 e^{-2id} - \frac{1}{4\pi^2}\Gamma^2 + \frac{1}{4\pi^2}\sum_{e=1}^{m+n} q_e^2 + \frac{1}{\pi}U_\infty e^{-id}\sum_{e=1}^{m+n}(a_e q_e + b_e q_e) + \frac{1}{\pi_i}U_\infty^{-id}\sum_{e=1}^{m+n}(a_e j_e - B_e j_e) + \frac{1}{2i\pi^2}\Gamma\sum_{e=1}^{m+n} q_e\right]\right\} \tag{14}$$

The real part of Eq. (14) is

$$M = \zeta\left\{2U_\infty^2\pi r^2 \sin 2\alpha + \frac{1}{2\pi}\Gamma\sum_{e=1}^{m+n} qe - U_\infty \cos\alpha \times \sum_{\ell=1}^{m+n}\left[q_\ell \sin\theta_\ell\left(Re + \frac{r^2}{R\ell}\right) - \gamma_\ell \sin\theta_\ell\left(R_\ell - \frac{r^2}{R_\ell}\right)\right] + U_\infty \times \sin\alpha \sum_{\ell=1}^{m+n}\left[q_\ell \cos\theta_\ell\left(Re + \frac{r^2}{R\ell}\right) + \gamma_\ell \sin\theta_\ell\left(R_\ell - \frac{r^2}{R\ell}\right)\right]\right\} \tag{15}$$

Substituting Eq. (4) into Eq. (12) yields

$$T = -\sum_{\ell=1}^{m+n} J_\ell \cos(\eta_\ell + \alpha)\,\mathrm{sgn}Q_\ell \tag{16}$$

Now set $m + n = 1$, $\mathrm{sgn}Q_1 = +1$, and $\pi/2 < (\eta_1 + \alpha) \le \pi$. Under these conditions, $T > 0$, i.e., the jet thrust is negative. This fact differs from the results of Spence[2] and Sedov[7] that the jet thrust does not depend on the jet escape angle. Instead, it coincides with the experimental data (for example, Refs. 4, 8, and 9), showing that if the jet-thrust coefficient c_J is not small, then the jet thrust is approximately proportional to $J\cos(\eta + \alpha)$. Here,

$$c_J = \frac{2J}{\rho U_\infty^2 c} \tag{17}$$

In the present case, $c = 4$, $r = 1$. Define the sum of all terms in Eq. (9) except the first one as the supercirculation $\Delta\Gamma$.

Taking into account that lift coefficient is

$$C_L = \frac{2L}{\rho U_\infty^2 c} \tag{18}$$

and recalling Eq. (13), the expression for the lift coefficient increment generated by supercirculation becomes

$$\Delta C_L = \frac{\Delta\Gamma}{U_\infty c} \tag{19}$$

where

$$C_L = C_{L0} + \Delta C_L \tag{20}$$

and C_{L0} is the lift coefficient not generated by supercirculation. Substituting $\Delta\Gamma$ from Eq. (9) into Eq. (19) and taking into account Eqs. (4), (5), and (17) yields

$$\Delta C_L = \sum_{\ell=1}^{m+n} c_{J\ell} \sin(\eta_\ell + \alpha)\,\mathrm{sgn}Q_\ell \frac{R_\ell^2 - r^2}{r^2 - 2rR_\ell\cos\theta_\ell + R_\ell^2} - \sum_{\ell=1}^{m+n} c_{J\ell}\cos(\eta_\ell + \alpha)\,\mathrm{sgn}Q_\ell \frac{2rR_\ell\sin\theta_\ell}{r^2 - 2rR_\ell\cos\theta_\ell + R_\ell^2} \tag{21}$$

In Eq. (21), the angles θ_ℓ in the plane $\zeta = \xi + i\psi$ correspond to the real nozzle locations on the airfoil. Equation (21) shows that the lift coefficient increment is linearly dependent on the jet thrust coefficient.

Radius R_ℓ is unknown and must be determined by an experiment in which the Bernoulli number [see Eq. (22) below] is equal to zero. This can be done by the use of Eq. (21) under conditions for which all the variables other than R_ℓ are known. When R_ℓ is defined, then the angles $(\eta_\ell + \alpha)$ and θ_ℓ can be chosen for the optimum lift and thrust for minimal takeoff and landing distances. Equation (21) has no extreme as a function of the two variables $(\eta_\ell + \alpha)$ and θ_ℓ, but if a value for one of these is chosen, then an extreme exists. At the same time, considering Eq. (21), it can be seen that both its terms with index ℓ are positive if, in the case of an escaping jet $0 < (\eta_\ell + \alpha) \le \pi/2$ and $-\pi < \theta_\ell < 0$; i.e., the jet has to escape downward from the airfoil bottom surface. This result coincides with the conclusion of Ref. 2 and with various experimental data. In the case of an entering jet, $-\pi/2 \le (\eta_\ell + \alpha) < 0$ and $0 < \theta_\ell < \pi$; i.e., the jet has to enter from the stream bottom part to the upper half of the airfoil leading edge. There is also the possibility that both terms of Eq. (21) can be positive if $-\pi < (\eta\ell + \alpha) \le -\pi/2$; $\pi < \theta_\ell < 0$.

It is interesting to note that, if $c_J \to \infty$, then the main items $\partial C_L/\partial\eta$ and $\partial C_L/\partial\alpha$ in Ref. 3 [see Eqs. (26) and (27)] have a linear dependence on c_J as well as in Eq. (21).

The method described above is suitable for entering jets and, if the difference between their Bernoulli constants and that of the freestream is small enough, for escaping jets.

Tangent Discontinuity Existing in Velocity at Boundaries

Now consider a case in which the jet Bernoulli constant is much higher than that of the freestream. In this case, with an ideal fluid, vortex sheets will occur on the boundaries between the jet and the stream. The vortex density on these sheets depends on Bernoulli number, a characteristic proposed by Shurigin,[5]

$$Be_\ell = \frac{2(b_\ell^* - B)}{\rho U_\infty^2} = \frac{V_{\infty\ell}^2}{U_\infty^2} - 1 \tag{22}$$

where b_ℓ^* is the Bernoulli constant of the jet and B that of the stream. The vortex density distribution on the upper and lower sheets depends also on the angle $(\eta_\ell + \alpha)$. To create a mathematical model of the flow under consideration, a source vortex of strength $(U_\infty^2/V_{\infty 2}^2)\gamma_2$ is placed at point A_2 (Fig. 2).

Here, γ_2 is defined according to Eq. (5). Now convert the boundary conditions between the jet and stream to linear ones as in Ref. 2, transferring the vortex sheet, the density of which is obtained as the difference between the densities of the upper and lower sheets, to the X axis (Fig. 2), since the angle α is small:

$$\int_{\frac{1}{2}}^{\infty} g_2(x)\,dx = \left(1 - \frac{U_\infty^2}{V_{\infty 2}^2}\right)\gamma_2 \tag{23}$$

Here, γ_2 is defined by Eq. (5) and $g_2(x)$ is the vortex density along the X axis, the distribution of which is assumed to be the same as in Ref. 2. The value of the integral in Eq. (23) is determined by the fact that only the difference between the verticle momentum components of the jet huber ℓ and that of another jet with the same initial angle and depth but without a discontinuity in the border velocity is matched by a lift generated with the aid of the velocity circulation on a path surrounding the vortex sheet. Since the jet thickness is finite in the present case, one of the propositions which Spence[2] made to obtain this distribution (namely, the constancy of the jet momentum flux) is, however, only approximately true.

To determine the source strength of the combined source vortex at point A_2, notice that ΔC_L depends on the real volume rate of flow of the jet. Therefore, the source strength as given in Eq. (4) is scaled down by the ratio $U_\infty/V_{\infty 2}$. Because of the linearity of the problem, superposition is used to obtain the lift of the plate with the source vortex and the semi-infinite vortex sheet. Thus, Eq. (21), with the ratio $U_\infty^2/V_{\infty 2}^2$ applied to its first term and the ratio $U_\infty/V_{\infty 2}$ applied to its second term, is used together with the equations of Ref. 3 for the vortex sheet to obtain the lift coefficient increment.

In Ref. 3, these equations are given in the following forms:

$$\frac{\partial C_L}{\partial \eta} = 2\sqrt{\pi} c_J (0.139 + 0.151 c_J^{-\frac{1}{2}} + c_J^{-1})^{\frac{1}{2}} \tag{24}$$

$$\frac{\partial C_L}{\partial \alpha} = 2\pi(1 + 0.151 c_J^{-\frac{1}{2}} + 0.219 c_J) \tag{25}$$

Observe that Eqs. (24) and (25) are the coefficients of the terms of an expansion C_L, specifically at η and α. Consequently, $2\pi(1...)$ in Eq. (25) is C_{L0} [see Eq. (20)]. Equations (24) and (25) are only approximations for numerical calculations carried out in Ref. 2. At $U_\infty \to 0$ and $c_{J\ell} \to \infty$, the lift of an airfoil with a jet does not exceed the jet momentum flux. The equality of these can be obtained only at $\eta + \alpha = \pi/2$ for an escaping jet and at $\eta + \alpha = -\pi/2$ for an entering jet. Consequently, the limit at $c_J \to \infty$ of the coefficients of c_J of unity power in Eqs. (24) and (25) must also be equal to unity (see also Ref. 10). Therefore, the following equation is used to replace Eq. (24):

$$\frac{\partial \Delta C_L}{\partial \eta} = \frac{\partial C_L}{\partial \eta} = 2\sqrt{\pi} c_J (0.08 + 0.34 c_J^{-\frac{1}{2}} + c_J^{-1})^{\frac{1}{2}} \tag{26}$$

Table 1 Singularity distance parameter

c_J	Be	U_∞	V_∞	k
4	888	12.24	365	4.61
3	651	12.24	316	3.58
2	443	12.24	258	3.00
1	221	12.24	182	2.38
0.5	110	30.6	322	1.95
0.25	51.6	30.6	228	1.65
0.05	10.1	30.6	102	1.27
0.005	0.11	30.6	32.25	1.05
0.004	−0.11	30.6	28.84	1.04
0.0005	−0.89	30.6	10.20	1.012

and instead of Eq. (25):

$$\frac{\partial C_L}{\partial \alpha} = 2\pi + 2\sqrt{\pi} c_J (0.08 + 0.34 c_J^{-\frac{1}{2}} + c_J^{-1})^{\frac{1}{2}} \tag{27}$$

Thus, for this case, the formula for the lift coefficient increment generated by supercirculation is

$$\Delta C_L = \frac{U_\infty^2}{V_\infty^2} c_J \sin(\eta + \alpha) \frac{k_2 - 1}{1 - 2k\cos\theta + k^2} - \frac{U_\infty}{V_\infty} c_J \cos(\eta + \alpha) \times \frac{2k \sin\theta}{1 - 2k\cos\theta + k^2} + \left(1 - \frac{U_\infty^2}{V_\infty^2}\right) c_J \sin(\eta + \alpha) 2\sqrt{\pi} \times \left\{0.08 + 0.34\left[c_J\left(1 - \frac{U_\infty^2}{V_\infty^2}\right)\right]^{-\frac{1}{2}} + \left[c_J\left(1 - \frac{U_\infty^2}{V_\infty^2}\right)\right]^{-1}\right\}^{\frac{1}{2}} \tag{28}$$

where $k = R/r$. In this formula, index ℓ is omitted as there is only one jet.

The quantity k can be determined by Eq. (28) if ΔC_L is known from an experiment in which the rest of the variables are fixed. This has been done using data from Refs. 8 and 9. These experiments used an elliptical profile of 203 mm chord and a slot width of 0.046 mm at the trailing edge ($\theta = 0$ deg) with $\eta = 31.4$ and 58.1 deg. The jet thrust coefficient range was 0–5 at Bernoulli numbers [see Eq. (22)] up to 890. The condition $\theta = 0$ requires that the second term of Eq. (28) must be zero and that the first term is in the form $[(K+1)/(K-1)]\sin(\eta + \alpha)$. Equation (26) was considered to be coincident with the experimental data. From the differences between Eqs. (26) and (28) with all the known variable values inserted, the quantity k was determined and is presented in Table 1. For jet thrust coefficients less than 0.005, Eq. (28) was used with $[1 - (U_\infty^2/V_\infty^2)]^{-\frac{1}{2}}$ and $[1 - (U_\infty^2/V_\infty^2)]^{-1}$ eliminated. The smaller the Bernoulli number, the closer k is to unity. In the experiments of Refs. 8 and 9, the jet thrust coefficient and Bernoulli number changed with time. Thus, the influence of each of them and of the angle θ is unknown. Therefore, in the last section of this work, $k = 2$ was used rather than $k = 3$ (compatible with c_J) or $k = 1.3$ (compatible with Bernoulli number) at the takeoff speed.

Equation (28) is one of the possible solutions to the problem formulated by Spence[2] for the flow over a plate with a jet, under the condition that the volume flow rate of the jet and the jet thickness are not zero.

Application of the Theory

Equation (20), where ΔC_L is determined according to Eq. (28), was chosen as the basis of aerodynamic characteristics calculations for a light STOL long-range (up to 7500 miles) canard aircraft. The takeoff weight was 840 kg, wing span 16 m, and main wing area 9.6 m^2. The jet of air emerged from an 80 mm wide slot along the entire span from the bottom wing surface with an angle of $0 \le \eta \le 90$ deg. (Here, η is equivalent to a jet flap deflection.)

The slot width was chosen from the consideration that an excessive jet velocity produces a low c_J and low thrust if the engine power is limited. Low c_J induces low lift. The low thrust increases takeoff distance; therefore, it is necessary to find an optimum Bernoulli number [Eq. (22)] for each design. Another important consideration for finding optimum conditions is the need to pass all the jet airflow through a root cross-section area of a wing surface and through a compressor in subsonic flow.

Coefficient C_{L0} was taken from Table 2 and is convenient for an ordinary wing. The radius R was taken as $2r$, which is close to that determined by the data of Ref. 2. The angle θ was taken as -30 deg. Takeoff power was 100 hp (73.6 kW) and 25% power failure at the critical point of the takeoff was

considered. The jet flow velocity was calculated from the formula

$$V_\infty^3 - V_\infty U_\infty^2 - \frac{150NK}{\rho h_\infty s} = 0 \tag{29}$$

where K was taken as 0.8. The jet thickness at infinity h_∞ was taken equal to the jet slot width.

Figure 3 shows C_L with and without 25% power failure (dotted lines), $c_{J+\infty}$ of the escaping jet with and without 25% power failure (dotted lines), $c_{J-\infty}$ of the entering jet with 25% power failure, and C_{Ln} the lift coefficient necessary for horizontal flight (Table 3). Figure 3 also shows C_L at $\eta = 25$ deg and $\alpha = 5$ deg as calculated by the use of Eqs. (24) and (25), which is the pure Spence[2] method. Figure 4 shows the jet thrust $T = J_{+\infty} - J_{-\infty}$ at $\eta + \alpha = 0$ with and without 25% power failure (dotted line).

Figure 5 shows the takeoff run with a wheel rolling coefficient $0.02 \le f \le 0.2$ and at $15 \le \eta + \alpha \le 75$ deg. This graph also shows the run of the same aircraft with a conventional flap deflected 15 deg at $f = 0.04$. The profile drag coefficient was taken from Table 2 and the total one is

$$c_D = c_{D0} + (C_L^2/\pi A) \tag{30}$$

Figure 6 shows the discontinued and continued takeoff distances. Discontinued takeoff includes the takeoff run, failure of one engine, and braking to a stop after 3 s delay. The continued takeoff includes the takeoff run, failure of one

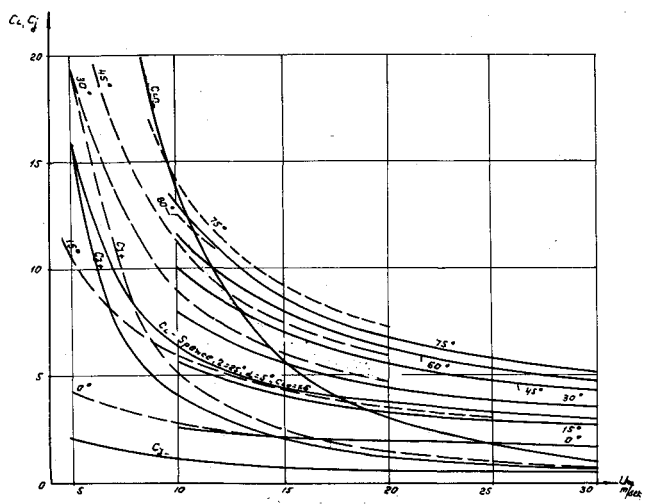

Fig. 3 Lift and jet thrust coefficients.

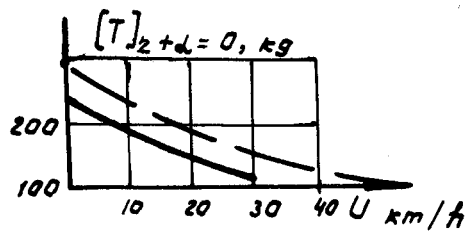

Fig. 4 Jet thrust.

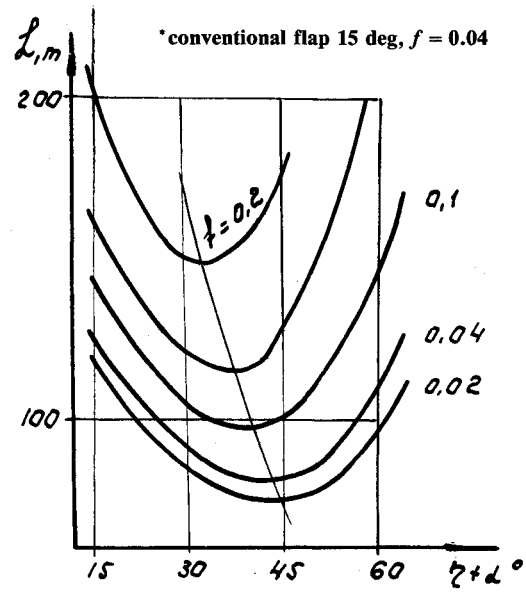

Fig. 5 Takeoff run.

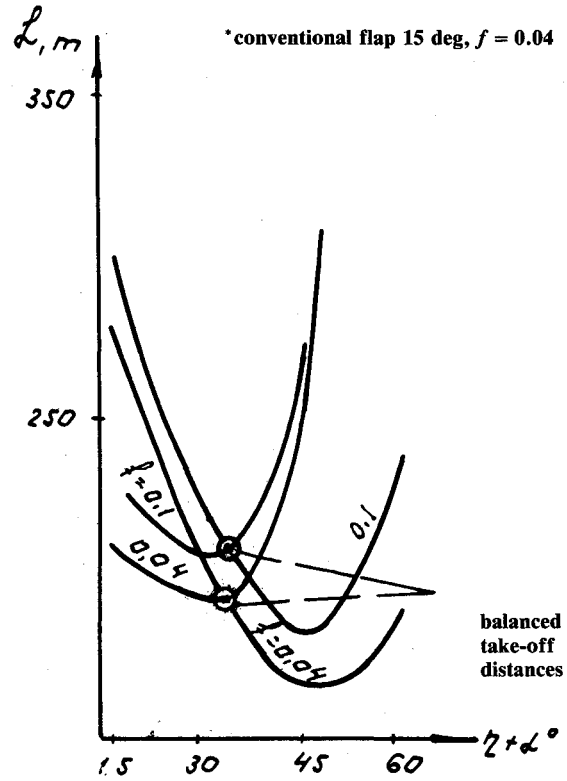

Fig 6 Takeoff distances.

Table 2 Initial lift and drag characteristics

$\eta + \alpha$, deg	C_{L0} max	c_{D0}	$\eta + \alpha$, deg	C_{LO} max	c_{D0}
0	1.2	0.015	60	2.0	0.035
15	1.4	0.02	75	2.2	0.04
30	1.6	0.025	90	2.5	0.045
45	1.8	0.03			

Table 3 Stall speed

$n + \alpha$, deg	U_{stall}, km/h	$\eta + \alpha$, deg	U_{stall}, km/h
0	88.6	45	45.5
5	84.2	60	41.0
15	68.0	75	37.2
30	54.7	90	36.8

engine at the instant of takeoff, and a climb to 30 ft for different $n + \alpha$ and f. Figure 6 also shows the balanced takeoff distance (distance of discontinued takeoff equal to distance of continued takeoff). One may observe that the optimum $\eta + \alpha$ is approximately 30 deg. The initial climb speed was chosen equal to the takeoff speed. It was calculated that this airspeed is 40 mph for $\eta = 25$ deg and $\alpha = 5$ deg, with the Bernoulli number equal to 14. For these cases, the thrust was calculated using the angle $\eta + \alpha$ (thrust recovery was not considered). The balanced takeoff distance is also shown for the same aircraft with a conventional flap, with an engine failure speed of 30 mph and with a takeoff airspeed of 65 mph. This distance is two times longer than that of the STOL version. If jet thrust recovery, which would occur at speeds greater than 37 mph, had been considered,[4] this result would have been a bit better. It would also be slightly better if radius R was taken as $1.3r$ in accordance with the Bernoulli number of 14.

Conclusions

In 1957, Spence[2] resolved the problem of the airfoil lift increment generated by an infinitely thin jet escaping from it. In this case, the jet flow rate equals zero, the Bernoulli number is infinite, and the horizontal projection of jet momentum does not generate a lift increment. The formation of such a jet requires infinite power. In practice, the need to obtain significant jet thrust with limited engine power leads to the use of a relatively slow jet with a significant flow rate. It is necessary to know the effect of such a jet on the lift increment and to determine the optimum jet parameters to minimize takeoff and landing distances.

In this paper, the lift increment generated by a jet of finite thickness is determined as the sum of two parts. The first is generated by a jet that has no discontinuities on the boundaries with the freestream, i.e., its Bernoulli number is zero. This component of the lift increment depends on both the horizontal and vertical projections of the jet momentum flux. The second component is that of Spence. Both are connected by means of coefficients depending on the Bernoulli number and the jet flow rate. The first component depends on various parameters, so that the radial location of the source vortex equivalent to the jet must be determined from experimental data. The present method is convenient for the preliminary design of STOL and V/STOL aircraft.

Acknowledgment

I am very grateful to Prof. Lazar E. Papernik of Boston University who has reviewed the paper and provided valuable comments and advice.

References

[1]Nekrasov, A. I., *Sobramie Sochineniy*, Academiya Nauk, Moscow, 1959, pp. 184–201.

[2]Spence, D. A., "Lift Coefficient of a Thin, Jet-Flapped Wing," *Proceedings of Royal Society of London*, Vol. 238A, 1956, pp. 46–68.

[3]Spence, D. A., "Some Simple Results for Two-Dimensional Jet-Flap Airfoils," *Aeronautical Quarterly*, Vol. 9, Nov. 1958, pp. 395–406.

[4]Bevilaqua, P. M., Shum, E. F., and Woam, C. J., "Progress Towards a Theory of Jet Flap Thrust Recovery," *Journal of Fluid Mechanics*, Vol. 141, April 1984, pp. 347–364.

[5]Shurigin, V. M., *Obtekanie tel so struyami*, Mashinostroenie, Moscow, 1977, pp. 1–200.

[6]Krassin, Y. A., "Hydrodynamicheskie Sili pri Istreihenii Strui v Snosiaschiy Potok," *Trudy GosNIIGA*, No. 165, Moscow, 1979, pp. 125–136.

[7]Sedov, L. I., *Mechanika Sploshnoy Sredi*, Vol. 2, Nauka, Moscow, 1973, pp. 80–85.

[8]Dimmock, N. A., "Some Early Jet Flap Experiments," *Aeronautical Quarterly*, Vol. 8, Nov. 1957, pp. 331–345.

[9]Dimmock, N. A., "Some Early Jet Flap Experiments, Some Further Jet Flap Experiments," Aeronautical Research Council, London, Current Papers 344 and 345, 1957.

[10]Krassin, Y. A., "O Hydrodynamicheskoi Reaktsii pri Besotrivnom Obtekanii Tela Struey Idealnoy Zidkosti," *Trudy GosNIIGA*, No. 86, Moscow, 1973, pp. 135–145.